THE JOURNAL OF PHYSICAL CHEMISTRY B

ARTICLE

pubs.acs.org/JPCB

Cu^{2+}-Induced Micellar Charge Selective Fluorescence Response of Acridine Orange: Effect of Micellar Charge, pH, and Mechanism

Amit K. Ghosh, Avik Samanta, and Prasun Bandyopadhyay*

Unilever R & D Bangalore, 64 Main Road, Whitefield, Bangalore-560066, India

Supporting Information

ABSTRACT:

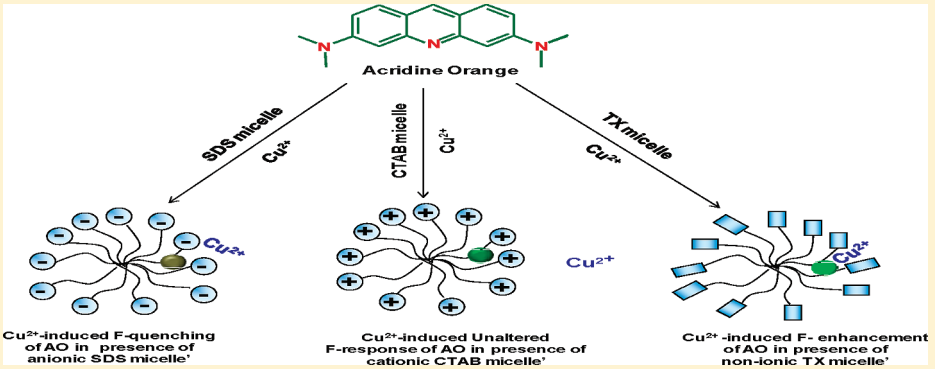

Photophysical properties of cationic Acridine Orange (AO) have been studied in different micellar environments [anionic SDS (sodium dodecyl sulfate), nonionic TX (TritonX-100), and cationic CTAB (cetyl trimethyl ammonium bromide)] at different pH, in the presence of a metal ion (Cu^{2+}). At pH ~ 8, addition of Cu^{2+} results in AO fluorescence quenching in the presence of SDS micelle, enhancement of the same in the presence of TX micelle, and remaining unaltered in the presence of CTAB micelle. At pH ~ 2, addition of Cu^{2+} results in AO fluorescence quenching only in the presence of SDS micelle, and it remains mostly unaffected in the presence of TX and CTAB. Availability of Cu^{2+} toward AO and binding of Cu^{2+} with AO at the charged micellar interface are responsible for this pH-dependent Cu^{2+}-mediated micellar charge selective fluorescence pattern.

INTRODUCTION

Fluorescence chemosensors are becoming increasingly popular due to their easy use in solution as well as for their high sensitivity and selectivity for some physiologically essential trace metal ions like Cu^{2+} and some hazardous metal species present in water like Pb^{2+}, As^{3+}, etc.[1−6] The merit of this sensor system lies in the selectivity and sensitivity of the system. A traditional approach to design new fluorescent sensors is synthetic modification of available dye molecules. This route is expensive and time consuming as well. Modern chemosensor research is aiming to tune the sensor power of nature-friendly probes by simple ways rather than synthesizing new sensor molecules. In recent times, there has been considerable interest to enhance the sensing capability of fluorescent chemosensors by noncovalent interaction with surfactant assemblies.[7−10] In a simple description, a fluorescence sensor system (receptor unit) needs two components, (i) an analyte and (ii) a transducer, which can translate the binding event of an analyte with the receptor unit in a readable manner. Surfactant micelles are well reported as a receptor system for various analytes (like protein, metal ions, etc.).[11,12] Fluorophore interactions with micelles and reverse micelles, which are the simplest mimics of membranes, are well studied in the literature.[13,14] Surfactants play an important role toward biosensor application because they stabilize intramolecular interactions of DNA−DNA and protein−protein molecules and also can solubilize the membrane proteins. The surfactant micelle is known to encapsulate the active components (like fluorophore, quencher, etc.) in the micellar nanocore, leads to enhanced communication between the active species, and improves sensory capability of the fluorophore.[10] Recently, we and other research groups have taken this advantage to develop a new class of fluorescent chemosensors with enhanced selectivity and sensitivity.[15−26]

Acridine Orange (AO) (pK_a ~ 10.4) exists in cationic form at pH < 10 and in completely deprotonated form at pH > 10.[27] The basic form can penetrate into the membrane of some cells by accepting protons, while the cationic form is not able to do so and therefore remains within the cell, which leads to the fluctuation in local ion concentration.[27] Systematic studies on the behavior of cationic AO in aqueous solution and its interaction with synthetic and biological systems has been a subject of interest for more than the last 50 years.[28−35] Liu and co-workers[36] have established

Received: July 13, 2011
Revised: September 2, 2011
Published: September 09, 2011

the method of determination of sodium carboxymethyl cellulose concentration in aqueous solution with the help of fluorescence quenching of AO. Gehlen and group[37] have reported fluorescence quenching of AO by aromatic amine molecules in the presence of cationic, anionic, and nonionic micelles. Copper is one of the essential trace metal ions present in biological systems and has been detected successfully through fluorescence sensing techniques.[38−40] Recently, we have reported that interaction of Cu^{2+} with AO leads to fluorescence quenching of the latter and helps to detect the former, and this fluorescence sensing (quenching) efficiency of AO was enhanced significantly in the presence of sodium dodecyl sulfate (SDS) micelle at pH ∼ 8.[41] In this study, we have used SDS micelle as a receptor unit, where fluorpohore AO (transducer) translates the binding event of the analyte (Cu^{2+}) with the receptor system (SDS micelle) in a readable manner through a change in fluorescence pattern. In the present study, we have varied the receptor system (anionic SDS micelle, cationic cetyl trimethyl ammonium bromide (CTAB) micelle, and nonionic TritonX-100 (TX) micelle) by keeping the transducer (AO) and analyte (Cu^{2+}) fixed. Here, we report micellar charge selective fluorescence response of cationic AO, in the presence of metal ion Cu^{2+} at various pH. The fluorescence intensity of AO quenched in the anionic SDS micellar nanocage remains unaffected in the presence of cationic CTAB micelle and is enhanced in the presence of nonionic TX micelle, at pH ∼ 8. The approachability of AO toward Cu^{2+} and a shift in monomer−dimer equilibrium of AO at the charged micellar environment are the determining factors for this observed micellar charge-selective pH-dependent fluorescence pattern of AO in the presence of Cu^{2+}. Thus, by utilizing this physical insight, one can exploit this fluorescence modulation technique to measure the concentration of the essential trace metal ions in biological environment.

EXPERIMENTAL SECTION

Materials. AO, SDS, TX, and CTAB were procured from Sigma-Aldrich Chemicals Co. $CuSO_4$, NaOH, and HCl were purchased from Merck. Water was obtained from a Milli-Q purification system. All experiments were performed with freshly prepared solutions.

METHODS

Fluorescence Study. All fluorescence studies were performed using a Shimadzu 5301 PC spectrophotometer at room temperature. The excitation wavelength for AO was set at 491 nm, and emission spectra were measured around 520 nm. The slit widths for both excitation and emission were set at 10 nm. For the fluorescence study in the presence of micelle, surfactant concentration kept constant above micellar concentration ([SDS] = 10 mM, [CTAB] = 1 mM, and [TX] = 0.5 mM) to ensure the presence of micelle under the experimental conditions. All solutions were prepared in Milli-Q water (conductance 2×10^{-6} S cm^{-1}), and all experiments were performed at room temperature. The pH of the solutions was adjusted by dilute HCl or dilute NaOH solution. To ensure the equilibrium, measurements were conducted after 24 h. Solutions were stored at room temperature and at atmospheric pressure. All the experiments were done in triplicate, and averages of those values are reported.

UV−vis Study. The UV−vis absorbance measurements were performed using a Perkin-Elmer Lambda 35 UV/vis spectrophotometer. Surfactant concentrations were above micellar concentration ([SDS] = 10 mM, [CTAB] = 1 mM, and [TX] = 0.5 mM) to ensure the presence of micelle under the experimental conditions. Absorbance values of the sample solutions were measured in the wavelength regime of 200−800 nm. All solutions were prepared in MQ water and mixed well before measurement. pH of the solutions was adjusted by dilute HCl or dilute NaOH. Experiments were carried out at room temperature, and measurements were taken in absorbance mode. All the experiments were done in triplicate, and averages of those values are reported.

Scheme 1. Molecular Structure of Acridine Orange (AO) (a) and Acridine (A) (b) Dye

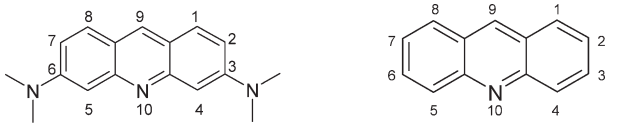

(a) (b)

RESULTS AND DISCUSSION

Recently we have reported[41] that at low pH (∼2) in a pure aqueous system Cu^{2+} acts as a quencher to the cationic AO, whereas at high pH (∼8) Cu^{2+} binds with AO and shifts its dimer−monomer equilibrium toward monomer (fluorophore), resulting in fluorescence intensity enhancement. AO can exist in monocationic, dicationic, and tricationic form, depending on medium pH.[42] The pK_a for monocation formation (protonation of ring nitrogen atom) is higher than that of dication and trication formation (protonation of $-NMe_2$ groups) (Scheme 1).[42] At low pH (∼2), AO exists in tricationic form, responsible for electrostatic repulsion between AO and Cu^{2+}. At pH ∼ 8, $-NMe_2$ groups of AO (monocationic AO) act as electron donors (as there is no possibility of protonation at pH ∼ 2) to the metal ion, and this complexation of AO (monomer) with Cu^{2+} leads to a shift in the dimer−monomer equilibrium toward its monomer side. It is reported[43] that at pH < 10 AO exists in cationic form, and this cationic AO can form a dimer when present in the high-concentration range (10^{-6}−10^{-4} M). Therefore, in our experimental conditions ([AO] = 10^{-6}−10^{-5} M and pH ∼ 2 to 8), AO is cationic and displays dimer−monomer equilibrium in solution.

Steady State Fluorescence Study of AO in the Presence of Anionic Micelle at Different pH. All fluorescence studies have been performed at a fixed concentration of AO (10^{-6} M). In Figure 1A, we have shown the change in fluorescence intensity of AO in the presence of SDS (10 mM) micelle at different Cu^{2+} concentrations, at pH ∼ 2. The fluorescence intensity of AO decreases with an increase in Cu^{2+} concentration. The result obtained upon addition of Cu^{2+} is in good agreement with the Stern−Volmer[44] equation, which can be expressed as follows

$$F_0/F = 1 + K_{SV}[Cu^{2+}] \quad (1)$$

F_0 and F are the fluorescence intensities of AO in the absence and presence of Cu^{2+}. The slope of the plot of F_0/F against $[Cu^{2+}]$ gives the Stern−Volmer quenching constant (K_{SV}), indicating the degree of sensitivity of the fluorophore for the detection of the metal ion. Fluorescence quenching of AO with Cu^{2+} gives K_{SV} of 0.15×10^3 M^{-1}. Again, at pH ∼ 8, addition of Cu^{2+} to the "AO−SDS" system (AO in the presence of 10 mM SDS) causes reduction in fluorescence intensity (Figure 1B), which follows

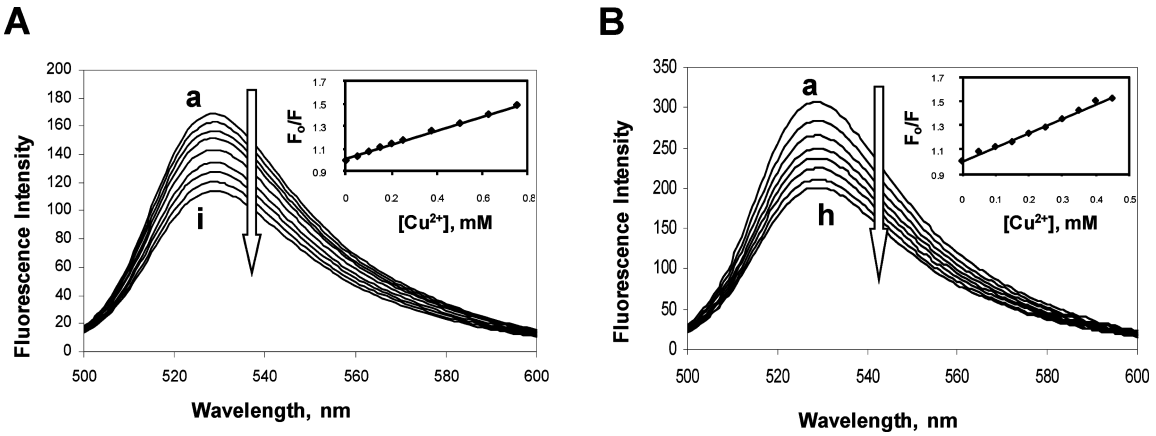

Figure 1. (A) Fluorescence emission of AO ([AO] = 10^{-6} M) in the presence of SDS micelle ([SDS] = 10 mM) with an increase in Cu^{2+} concentration, at pH ∼ 2, where Cu^{2+} varied from 0 mM (a) to 0.75 mM (i). (B) Fluorescence emission of AO ([AO] = 10^{-6} M) in the presence of SDS micelle ([SDS] = 10 mM) with an increase in Cu^{2+} concentration, at pH ∼ 8, where Cu^{2+} varied from 0 mM (a) to 0.45 mM (i). Inset: Plot of F_0/F vs [Cu^{2+}] (Stern−Volmer plot) for the AO−SDS micelle system.

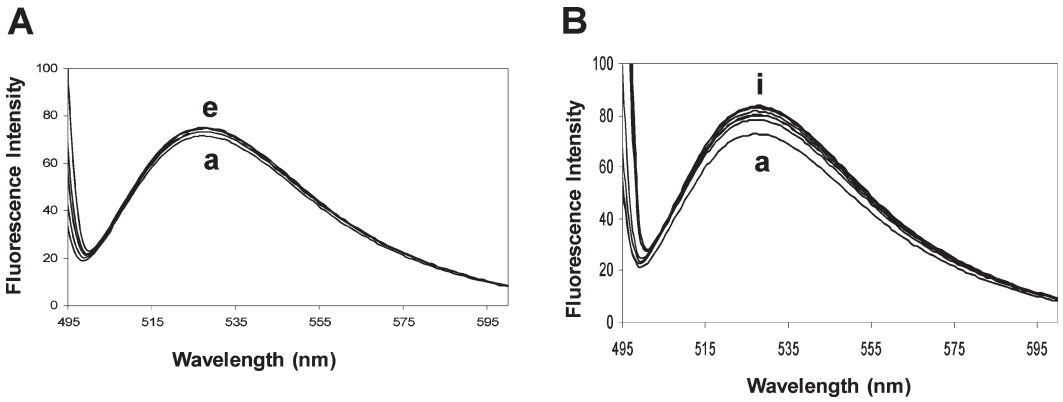

Figure 2. (A) Fluorescence emission of AO ([AO] = 10^{-6} M) in the presence of CTAB micelle ([CTAB] = 1 mM) with increase in Cu^{2+} concentration, at pH ∼ 2, where Cu^{2+} varied from 0 mM (a) to 17.5 mM (e). (B) Fluorescence emission of AO ([AO] = 10^{-6} M) in the presence of CTAB micelle ([CTAB] = 1 mM) with increase in Cu^{2+} concentration, at pH ∼ 8, where Cu^{2+} varied from 0 mM (a) to 20 mM (i).

the Stern−Volmer equation, where the K_{SV} value is 1.21×10^3 M^{-1}. This K_{SV} value at pH ∼ 8 is higher than that at pH ∼ 2. In our earlier work,[41] we have explained that this higher K_{SV} value (in the presence of SDS micelle) is a result of enhanced communication between AO and Cu^{2+} at the micelle−water interface and depends on cationic charge density of AO−monomer and the availability of AO−monomer at the SDS micelle−water interface. The higher cationic charge density on AO at pH ∼ 2 hinders the approachability of Cu^{2+} toward AO in comparison to the same at pH ∼ 8, and this could be the possible reason for the low K_{SV} value at pH ∼ 2 compared to pH ∼ 8. Quenching of AO (10^{-6} M) fluorescence starts at the Cu^{2+} concentration as low as 75 μM, at pH ∼ 8.

Steady State Fluorescence Study of AO in the Presence of Cationic Micelle at Different pH. In Figure 2, we have shown the change in fluorescence intensity of AO in the presence of cationic CTAB micelle, which remains unaltered with increasing [Cu^{2+}] at pH ∼ 2 and holds true even at higher pH (∼8). Fluorescence intensity of AO in the presence of Cu^{2+} is governed by the extent of interaction between these two active species (AO and Cu^{2+}), which depends on the approachability between them in the presence of charged micelle. CTAB is a cationic surfactant, where cationic charge at the micelle−water interface may hinder the approachability of the metal cation (Cu^{2+}) toward the CTAB micelle, hence the approachability toward AO (present in the CTAB micelle−water interface). This electrostatic repulsion between cationic micelle and metal ion Cu^{2+} could be the possible reason for unaltered fluorescence response (irrespective of pH) of AO (in CTAB micelle) with progressive increase in [Cu^{2+}].

Steady State Fluorescence Study of AO in the Presence of Nonionic Micelle at Different pH. The most interesting phenomena are the fluorescence responses of AO in the presence of nonionic TX micelle, at different pH. In Figure 3A, we have shown that at pH ∼ 2 the fluorescence intensity of AO in the presence of TX micelle remains unchanged with an increase in [Cu^{2+}]. This could be due to lack of preferential binding sites of nonionic micelle TX which is unable to bring tricationic AO and Cu^{2+} close enough to interact.

However, at pH ∼ 8, addition of Cu^{2+} in the AO−TX micelle system causes enhancement in fluorescence intensity (Figure 3B). The unprotonated AO monomer at this pH can bind with Cu^{2+} in the polyoxyethylene chain of TX due to enough water penetration and thus probably shifts the dimer−monomer equilibrium toward the monomer side of AO. Quenching of AO (10^{-6} M) fluorescence starts at the Cu^{2+} concentration as low as 25 μM, at pH ∼ 8.

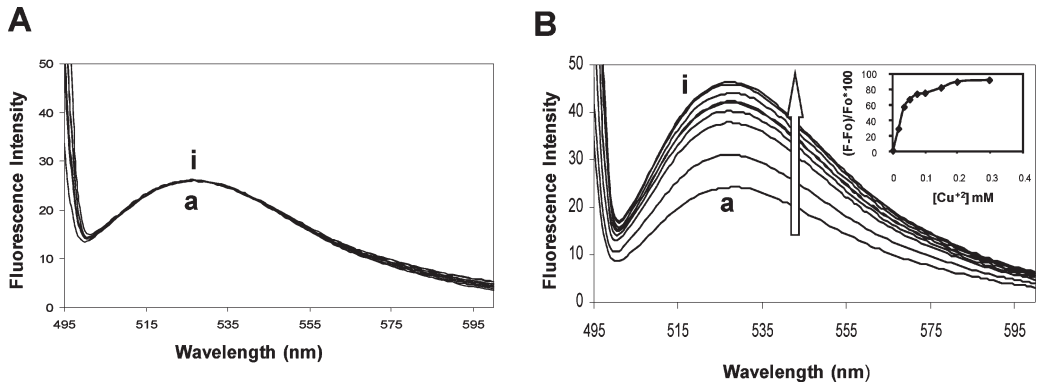

Figure 3. (A) Fluorescence emission of AO ([AO] = 10^{-6} M) in the presence of TX micelle ([TX] = 0.5 mM) with an increase in Cu^{2+} concentration, at pH ~ 2, where Cu^{2+} varied from 0 mM (a) to 3 mM (i). (B) Fluorescence emission of AO ([AO] = 10^{-6} M) in the presence of TX micelle ([TX] = 0.5 mM) with an increase in Cu^{2+} concentration, at pH ~ 8, where Cu^{2+} varied from 0 mM (a) to 0.3 mM (i). Inset: plot of percentage increment of fluorescence ($[F - F_0]/F_0 \times 100$) of the AO−TX micelle system with $[Cu^{2+}]$, at pH ~ 8.

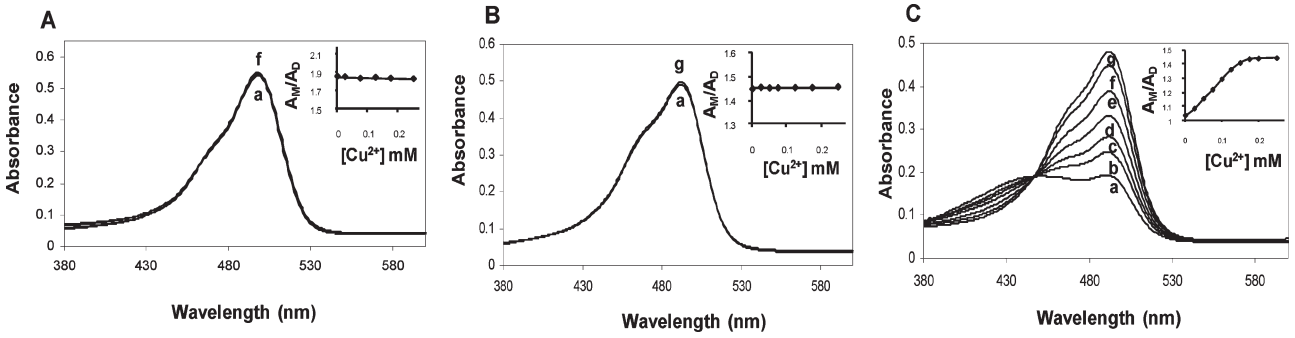

Figure 4. (A) UV−vis spectra of the AO−SDS micelle system with progressive addition of Cu^{2+}, at pH ~ 8. Here Cu^{2+} varied from 0 (a) to 0.27 (g) mM, [AO] = 10^{-6}, [SDS] = 10 mM. (B) UV−vis spectra of the AO−CTAB micelle system with progressive addition of Cu^{2+}, at pH ~ 8. Here Cu^{2+} varied from 0 (a) to 0.27 (g) mM, [AO] = 10^{-6}, [CTAB] = 0.1 mM. (C) UV−vis spectra of the AO−TX micelle system with progressive addition of Cu^{2+}, at pH ~ 8. Here Cu^{2+} varied from 0 (a) to 0.27 (g) mM, [AO] = 10^{-6}, [TX] = 0.2 mM. Inset: Plot of A_M/A_D vs $[Cu^{2+}]$ for the respective system, where A_M and A_D are the absorbance at 492 (for monomer) and 465 (dimer), respectively.

UV−vis Study of AO in the Presence of Different Micelles (SDS, TX, and CTAB). To investigate the validity of this hypothesis (micellar charge based fluorescence response of AO in the presence of Cu^{2+}), we have monitored the change in UV−vis spectra of AO in the presence of different micellar environments (SDS, CTAB, and TX) with progressive addition of Cu^{2+} (Figure 4), at pH ~ 8. It is reported in the literature[43] that the absorption peak of the AO monomer appears at ~491 nm, and the dimer peak appears as a left shoulder peak at ~465 nm. Addition of Cu^{2+} to the AO in the presence of anionic SDS and cationic CTAB micelle does not affect the absorbance profile of AO, whereas in the presence of nonionic TX micelle the absorbance value at ~491 increases with an increase in $[Cu^{2+}]$. We have already established that at pH ~ 8, in the absence of micelle (pure aqueous system), $-NMe_2$ groups of AO (monocationic AO) can act as electron donors (as there is no possibility of protonation like at pH ~ 2) to Cu^{2+}, leading to AO (monomer) complexation with Cu^{2+}, which results in a dimer−monomer equilibrium shift toward the monomer (fluorophore) side and an increase in AO fluorescence intensity.[41] To verify this possibility (shift in dimer−monomer equilibrium after addition of Cu^{2+}, at pH ~ 8), in the presence of micelle, we have plotted (Figure 4 insets) the change in ratio (A_M/A_D) of monomer absorbance (A_M) to the dimer absorbance (A_D) with Cu^{2+} concentration (in the presence of charged micelle), by assuming that the amount of monomer or dimer present in the solution phase will be proportional to the absorbance value of the respective species. In the case of TX, absorbance at 491 and the A_M/A_D ratio are found to increase with $[Cu^{2+}]$, whereas both remain unaltered in the presence of anionic SDS and cationic CTAB micelle. This observation reflects that, in the presence of nonionic TX, micelle addition of Cu^{2+} to the AO leads to more AO monomer formation (shift of AO dimer−monomer equilibrium toward monomer direction), whereas in the presence of SDS and CTAB micelle, the AO dimer−monomer equilibrium remains unaffected after addition of Cu^{2+}.

Distribution of AO Monomer/AO Dimer in the Micelle (SDS, CTAB, and TX) and Cu^{2+} Sensitivity at pH ~ 8. Interaction between AO and Cu^{2+} at the charged micelle−water interface depends on the heterogeneous distribution of AO in the inter phase. Distribution of AO is expected to be different in the presence of different charged (SDS and CTAB) and uncharged micelles (TX). Poisson statistics can be used to determine the distribution of AO within the micellar solution.[45,46] Solubilization or distribution of AO in the water and micellar phase is expected to be in the following equilibrium

$$[AO^{water}] + M \overset{K}{\leftrightarrow} [AO^{micelle}] \quad (1)$$

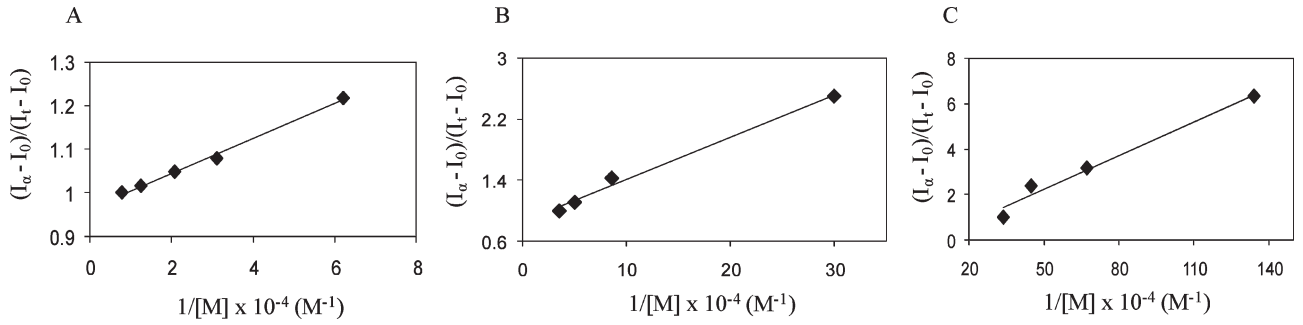

Figure 5. Binding curve of AO (10^{-6} M) with (A) SDS micelle, (B) CTAB micelle, and (C) TX micelle, at pH ~ 8.

Table 1. Distribution of AO (10^{-6} M) in the Different Charged Micelles (SDS, CTAB, and TX), at pH ~ 8

	A_M/A_D	AO_M (M)	AO_D (M)	K (M^{-1})	$AO_M^{Micelle}$ (M)	AO_M^{Water} (M)
SDS	1.98	6.64×10^{-7}	3.36×10^{-7}	24.88×10^4	6.13×10^{-7}	5.09×10^{-8}
CTAB	1.45	5.91×10^{-7}	4.09×10^{-7}	18.08×10^4	2.22×10^{-7}	3.51×10^{-7}
TX	1.03	5.08×10^{-7}	4.92×10^{-7}	20.12×10^4	1.58×10^{-7}	3.99×10^{-7}

According to this distribution, the concentration of AO in the water phase is

$$[AO^{water}] = [AO]/(1 + K[M]) \quad (2)$$

and the concentration of AO in the micellar phase is

$$[AO^{micelle}] = K[M][AO]/(1 + K[M]) \quad (3)$$

where [AO] is the total concentration of acridine orange, [M] is the concentration of micelles, and K is the binding constant of AO with the charged micelle.

The concentration of micelles [M] is determined by the following equation[47]

$$[M] = ([S] - CMC)/N_{agg} \quad (4)$$

where [S] is the total surfactant concentration; CMC is the critical micellar concentration of the respective surfactant; and N_{agg} is the aggregation number of the surfactant micelle (62 for SDS, 60 for CTAB, and 134 for TX).[48,49]

K can be obtained from the following relation[45]

$$(I_\alpha - I_O)/(I_t - I_O) = 1 + 1/K[M] \quad (5)$$

where I_α, I_t, and I_O are the fluorescence intensity at complete solubilization, at intermediate surfactant concentration, and in the absence of surfactant, respectively.

The plots of $(I_\alpha - I_O)/(I_t - I_O)$ against 1/[M] have been found to be linear (Figure 5), in accordance with eq 4. The binding constant (K) values have been determined from the slopes of the individual plots. Determination of this binding constant is based on the change in fluorescence intensity of AO in the presence and absence of surfactant. AO can present in both monomer and dimer form in the micellar solution, where the AO monomer (AO_M) is a fluorophore but the AO dimer (AO_D) is not. Therefore, the binding constant determined based on this process gives information about the binding of the AO monomer with the surfactant micelle, not about the binding of the AO dimer with the surfactant micelle. On the basis of this binding constant (K) of the AO monomer with the surfactant micelle, it is possible to determine the distribution of the AO monomer in the water and micellar phase (by replacing [AO] with $[AO_M]$ in eqs 1 and 2).

The concentration of the AO monomer in the water phase is

$$[AO_M^{water}] = [AO_M]/(1 + K[M]) \quad (6)$$

The concentration of the AO monomer in the micellar phase is

$$[AO_M^{micelle}] = K[M][AO_M]/(1 + K[M]) \quad (7)$$

The total amount of AO present in the micellar solution exists in monomer or in dimer form. Therefore, $[AO_M]$ can be obtained with the help of the following equation and $[AO_M]/[AO_D]$ ratio.

$$[AO] = [AO_M] + [AO_D] \quad (8)$$

$[AO_M]/[AO_D]$ is the ratio of concentration of the AO monomer to concentration of AO dimer. This is obtained from the ratio of absorbance of the AO monomer (at 491 nm) to absorbance of the AO dimer (at 465 nm), in the presence of different charged micelles (Supporting Information), by assuming the amount of monomer or dimer present in the micellar solution will be proportional to the absorbance value of the respective species.[41] Results obtained based on Poisson distribution are summarized in Table 1. It is evident that the availability of the AO monomer (fluorophore) is less because of a partition of AO as monomer and dimer and a further partition of the AO monomer in the micellar and water phase. This less availability of fluorophore (AO monomer) at the micellar interface could be the reason for the low sensitivity of the present system. To check this hypothesis, we have performed a fluorescence quenching study at a higher concentration of AO (10^{-5} M), at pH ~ 8 (Figure 6). Although the fluorescence pattern remains the same for different surfactant micelles, we have observed improvement in the sensor capability of this system. Now only 12.5 μM Cu^{2+} is required for SDS micelle and 5.0 μM Cu^{2+} is required for TX micelle. These results indicate that the sensitivity of the present system can be fine-tuned by varying the availability of the AO monomer at the micelle−water interface.

Mechanism of Cu^{2+}-Induced Micellar Charge Selective Fluorescence Response of AO at pH ~ 8. Cationic AO displays "dimer−monomer" equilibrium under the experimental conditions ([AO] ~ 10^{-5} M and 10^{-6} M and pH ~ 2−8). The fluorescence

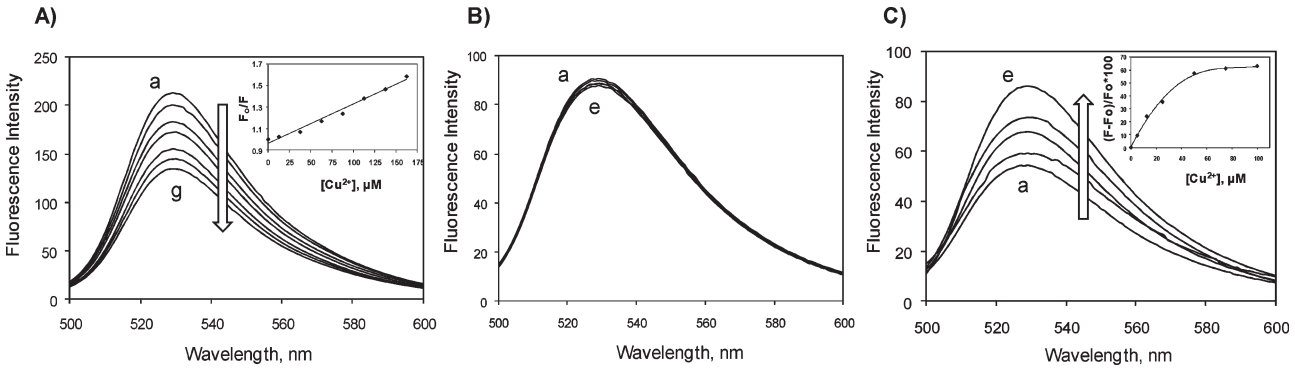

Figure 6. (A) Fluorescence emission of AO ([AO] = 10^{-5} M) in the presence of SDS micelle ([SDS] = 10 mM) with an increase in Cu^{2+} concentration, at pH ~ 8, where Cu^{2+} varied from 0 μM (a) to 170 μM (g). Inset: Plot of F_0/F vs [Cu^{2+}] (Stern−Volmer plot). (B) Fluorescence emission of AO ([AO] = 10^{-5} M) in the presence of CTAB micelle ([CTAB] = 1 mM) with an increase in Cu^{2+} concentration, at pH ~ 8, where Cu^{2+} varied from 0 mM (a) to 300 μM (e). (C) Fluorescence emission of AO ([AO] = 10^{-5} M) in the presence of TX micelle ([TX] = 0.5 mM) with an increase in Cu^{2+} concentration, at pH ~ 8, where Cu^{2+} varied from 0 mM (a) to 100 μM (e). Inset: plot of percentage increment of fluorescence ($[F - F_0]/F_0 \times 100$) with [Cu^{2+}], at pH ~ 8.

Scheme 2. Proposed Mechanism for Interaction of AO with a Metal Ion (Cu^{2+}) in the Presence of Charged Micelle: Location of AO (Dark Green ≈ Quenched AO, Green ≈ Unaffected AO, and Bright Green ≈ Fluorescent AO)

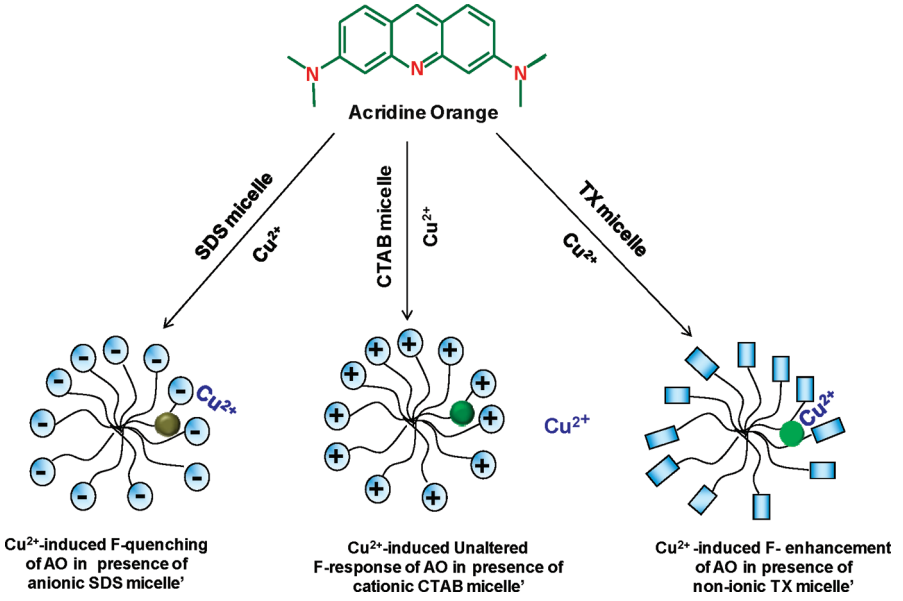

response of AO depends on two major factors: first, a shift in dimer−monomer equilibrium of AO and second, fluorescence quenching of the AO monomer. An UV−vis study confirms that in the presence of anionic SDS micelle AO dimer−monomer equilibrium remains unaffected after addition of Cu^{2+}. Moreover, quenching in fluorescence intensity of AO in the presence of SDS micelle (after addition of Cu^{2+}) is in accordance with the Stern−Volmer equation. These two observations suggest that a decrease in fluorescence intensity of AO (after addition of Cu^{2+}) in the presence of anionic SDS micelle is a result of fluorescence quenching, not because of a shift in dimer−monomer equilibrium (Scheme 2). Again, in the presence of a cationic CTAB micelle, both fluorescence intensity and AO dimer−monomer equilibrium remain unaffected (after addition of Cu^{2+}), which suggests that electrostatic repulsion between the cationic micelle (CTAB) and Cu^{2+} inhibits the approachability of Cu^{2+} toward the AO (present in the micellar core), responsible for the unaltered absorbance and fluorescence pattern of AO in the presence of a CTAB micelle (Scheme 2). Interestingly, in the presence of a nonionic TX micelle, both fluorescence intensity and absorbance at ~491 increase with an increase in [Cu^{2+}]. The UV−vis study reveals that addition of Cu^{2+} to the "AO−TX micelle" leads to AO−Cu^{2+} complex formation at the micelle−water interface, which results in a shift of AO dimer−monomer equilibrium toward the monomer side. All these facts suggest that addition of Cu^{2+} in the AO−TX micelle system leads to more AO monomer (fluorophore) formation, responsible for enhancement of fluorescence intensity of AO in the presence of the TX micelle (after addition of Cu^{2+}) at pH ~ 8 (Scheme 2).

Finally, the effects of the $-NMe_2$ groups of AO have been investigated toward fluorescence activity. Molecular structure (Scheme 1) of acridine (A) is quite similar with that of AO, except $-NMe_2$ substations at the 3 and 6 positions are lacking for A. The fluorescence intensity change of both the dyes

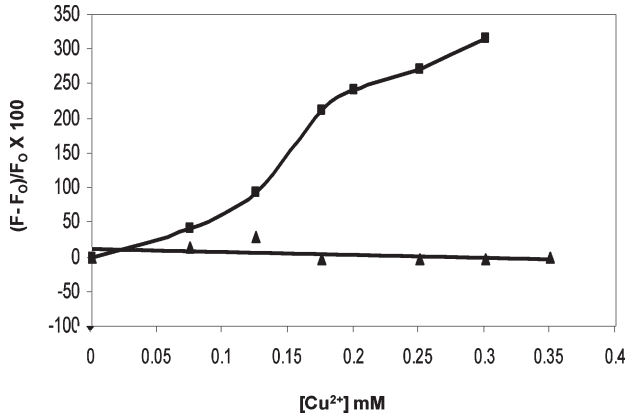

Figure 7. Percentage increment of fluorescence intensity ($[F - F_0]/F_0 \times 100$) of AO (■) and A (▲) with $[Cu^{2+}]$ at pH ∼ 8.

(AO and A) in the presence of transition metal ion Cu^{2+}, at pH ∼ 8, has been studied. Fluorescence intensity changes have been plotted in Figure 7 as a percentage increment of intensity $[(F - F_0)/F_0 \times 100]$, where F_0 and F are the fluorescence intensity of the fluorophore in the absence and presence of Cu^{2+}. Here, progressive addition of Cu^{2+} (at pH ∼ 8) causes an increase in fluorescence intensity of AO, keeping the intensity of A almost unchanged, proving the point that $-NMe_2$ groups at the 3 and 6 position of the AO molecule are particularly responsible for fluorescence change. This could be due to complex formation between Cu^{2+} and AO at pH ∼ 8, which is not possible at pH ∼ 2 due to protonation of $-NMe_2$ groups.

CONCLUSION

In summary, we have shown that the Cu^{2+}-induced fluorescence pattern of AO in the presence of micelle is selective to the micellar charge and pH of the system. At pH ∼ 8, Cu^{2+} causes a reduction in fluorescence intensity (fluorescence quenching) of AO in the presence of anionic SDS micelle, and the same remains unaltered in the presence of cationic CTAB micelle. Interestingly, at the same pH, AO fluorescence intensity was enhanced with an increase in Cu^{2+} concentration in nonionic TX micellar environment, due to a shift in the AO dimer−monomer equilibrium toward the AO monomer side. This physical insight of the micellar charge dependent fluorescence pattern of AO in the presence of Cu^{2+} has a high potential to either modify the existing micelle based fluorescent chemosensors or develop new fluorescent chemosensors. The sensitivity of the present system can be fine-tuned by varying the availability of the AO monomer at the micelle−water interface.

ASSOCIATED CONTENT

Supporting Information. UV−vis spectroscopy of AO in the absence and presence of SDS, CTAB, and TX micelle and binding curve for AO with SDS, CTAB, and TX micelle at pH ∼ 2. This material is available free of charge via the Internet at http://pubs.acs.org.

AUTHOR INFORMATION

Corresponding Author

*E-mail:prasun.bandyopadhyay@unilever.com. Tel.: +91-080-398-30992. Fax: +91-080-2845-3086.

ACKNOWLEDGMENT

A.S. thanks Unilever R&D Bangalore, India, for the support via a summer research project. Authors would like to acknowledge one of the anonymous reviewers for constructive criticism and suggestions of the manuscript.

REFERENCES

(1) De Silva, A. P.; Fox, D. B.; Huxley, A.J.M.; Moody, T. S. *Coord. Chem. Rev.* **2000**, *205*, 41–57.
(2) Amendola, V.; Fabbrizzi, L.; Licchelli, M.; Mangano, C.; Pallavicini, P.; Parodi, L.; Poggi, A. *Coord. Chem. Rev.* **1999**, *192*, 649–669.
(3) Mameli, M.; Aragoni, M. C.; Arca, M.; Caltagirone, C.; Demartin, F.; Farruggia, G.; Filippo, G. D.; Devillanova, F. A.; Garau, A.; Isaia, F.; Lippolis, V.; Murgia, S.; Prodi, L.; Pintus, A.; Zaccheroni, N. *Chem.—Eur. J.* **2010**, *16*, 919–930.
(4) McCoy, C. P.; Rademacher, J. T.; Rice, T. E. *Chem. Rev.* **1997**, *97*, 1515–1566.
(5) Hirano, T.; Kikuchi, K.; Urano, Y.; Higuchi, T.; Nagano, T. *J. Am. Chem. Soc.* **2000**, *122*, 12399–12400.
(6) Spichiger-Keller, U. E. *Chemical Sensors and Biosensors for Medical and Biological Applications*; Wiley-VCH: Berlin, 1998.
(7) Mallick, A.; Mandal, M. C.; Haldar, B.; Chakraborty, A.; Das, P.; Chattopadhyay, N. *J. Am. Chem. Soc.* **2006**, *128*, 3126–3127.
(8) Chakraborty, A.; Mallick, B.; Haldar; Purkayastha, P.; Das, P.; Chattopadhyay, N. *Langmuir* **2007**, *23*, 4842–4848.
(9) Ghosh, A. K.; Bandyopadhyay, P. *Chem. Commun.* **2011**, *47*, 8937–8939.
(10) Pallavicini, P.; Diaz-Fernandez, Y. A.; Pasotti, L. *Coord. Chem. Rev.* **2009**, *253*, 2226–2240.
(11) Bandyopadhyay, P.; Ghosh, A. K. *Sens. Lett.* **2011**, *9*, 1249–1264.
(12) González, D. C.; Savariar, E. N.; Thayumanavan, S. *J. Am. Chem. Soc.* **2009**, *131*, 7708–7716.
(13) Panda, D.; Khatua, S.; Datta, A. *J. Phys. Chem. B* **2006**, *110*, 2611–2617.
(14) Mallick, A.; Haldar, B.; Maiti, S.; Chattopadhyay, N. *J. Colloid Interface Sci.* **2004**, *278*, 215–223.
(15) Bandyopadhyay, P.; Saha, K. *Chem. Phys. Lett.* **2008**, *457*, 227–231.
(16) Bandyopadhyay, P.; Joseph, M. T. *Anal. Biochem.* **2010**, *397*, 89–95.
(17) Bandyopadhyay, P.; Ghosh, A. K.; Bandyopadhyay, S. *Chem. Phys. Lett.* **2009**, *476*, 244–248.
(18) Bandyopadhyay, P.; Ghosh, A. K. *J. Phys. Chem. B* **2009**, *113*, 13462–13464.
(19) Bandyopadhyay, P.; Ghosh, A. K. *J. Phys. Chem. B* **2010**, *114*, 11462–11467.
(20) Das, P.; Mallick, A.; Sarkar, D.; Chattopadhyay, N. *J. Colloid Interface Sci.* **2008**, *320*, 9–14.
(21) Riis-Johannessen, T.; Severin, K. *Chem.—Eur. J.* **2010**, *16*, 8291–8295.
(22) Chirico, G.; Collini, M.; D'Alfonso, L.; Denat, F.; Diaz-Fernandez, Y. A.; Pasotti, L.; Rousselin, Y.; Sok, N.; Pallavicini, P. *ChemPhysChem.* **2008**, *9*, 1729–1737.
(23) Denat, F.; Diaz-Fernandez, Y. A.; Pasotti, L.; Sok, N.; Pallavicini, P. *Chem.—Eur. J.* **2010**, *16*, 1289–1295.
(24) Mameli, M.; Aragoni, M. C.; Arca, M.; Caltagirone, C.; Demartin, F.; Farruggia, G.; Filippo, G. D.; Devillanova, F. A.; Garau, A.; Isaia, F.; Lippolis, V.; Murgia, S.; Prodi, L.; Pintus, A.; Zaccheroni, N. *Chem.—Eur. J.* **2010**, *16*, 919–930.
(25) Iatridi, Z.; Bokias, G. *Langmuir* **2008**, *24*, 11506–11513.
(26) Iatridi, Z.; Daktiloudis, A.; Bokias, G. *Polym. Int.* **2010**, *59*, 1168–1174.
(27) Falcone, R. D.; Correa, N. M.; Biasutti, M. A.; Silber, J. J. *Langmuir* **2002**, *18*, 2039–2047.
(28) Z Zanker, V. Z. *Phys. Chem.* **1952**, *199*, 225–234.

(29) Vitagliano,V. In *Aggregation Processes in Solution*; Wyn-Jones, E., Gormally, J., Eds.; Elsevier: Amsterdam, 1983; pp 271−308.
(30) Schreiber, J. P.; Daune, M. P. *J. Mol. Biol.* **1974**, *83*, 487–501.
(31) Guo, X.-Q.; Zhang, Z.-L.; Zhao, Y-B .; Wangs, D.-Y.; Xu, J.-G. *Appl. Spectrosc.* **1997**, *51*, 1002–1007.
(32) Zimmermann, F.; Hossenfelder, B.; Panitz, J. C.; Wokaun, A. *J. Phys. Chem.* **1994**, *98*, 12796–12804.
(33) Clerc, S.; Barenholdz, Y. *Anal. Biochem.* **1998**, *259*, 104–111.
(34) Brauns, E. B.; Murphy, J. C.; Berg, M. A. *J. Am. Chem. Soc.* **1998**, *120*, 2449–2456.
(35) Davies, D. B.; Veselkov, D. A.; Kodintsev, V. V.; Evstigneev, M. P.; Veselkov, A. N. *Mol. Phys.* **2000**, *98*, 1961–1971.
(36) Liu, S. P.; Sa, C.; Hu, X. L.; Kong, L. *Spectrochim. Acta, Part A.* **2006**, *64*, 817–822.
(37) Gehlen, M. H.; Fo, P. B.; Neumann, M. G. *J. Photochem. Photobiol. A: Chem.* **1991**, *59*, 335–340.
(38) Li, P.; Duan, X.; Chen, Z.; Liu, Y.; Xie, T.; Fang, L.; Li, X.; Yin, M.; Tang, B. *Chem. Commun.* **2011**, *47*, 7755–7757.
(39) Taki, M.; Iyoshi, S.; Ojida, A.; Hamachi, I.; Yamamoto, Y. *J. Am. Chem. Soc.* **2010**, *132*, 5938–5939.
(40) Wu, S.-P.; Wang, T.-H.; Liu, S.-R. *Tetrahedron.* **2010**, *66*, 9655–9658.
(41) Ghosh, A. K.; Samanta, A.; Bandyopadhyay, P. *Chem. Phys. Lett.* **2011**, *507*, 162–167.
(42) Schuleman, S. G.; Naik, D. V.; Capomacchia, A. C.; Roy, T. *J. Pharm. Sci.* **1975**, *64*, 982–986.
(43) Luo, Y. J.; Shen, H. X. *Anal. Commun.* **1999**, *36*, 135–137.
(44) Lakowicz, J. R. *Principles of Fluorescence Spectroscopy*; Plenum: New York, 1999.
(45) Almgren, M.; Grieser, F.; Thomas, J. K. *J. Am. Chem. Soc.* **1979**, *101*, 279.
(46) Yekta, A.; Aikawa, M.; Turro, N. J. *Chem. Phys. Lett.* **1979**, *63*, 543.
(47) Quina, F. H.; Toscano, G. *J. Phys. Chem.* **1977**, *81*, 1750.
(48) Saroja, G.; Ramachandan, B.; Saha, S.; Samanta, A. *J. Phys. Chem. B* **1999**, *103*, 2906.
(49) Phillies, G. D. J.; Stott, J.; Ren, S. Z. *J. Phys. Chem.* **1993**, *97*, 11563.